

# Adsorption Performance of Hollow Spherical Sludge Carbon Prepared from Sewage Sludge and Polystyrene Foam Wastes

Zhijian Wu,<sup>†,‡</sup> Lingjun Kong,<sup>†,§</sup> Hang Hu,<sup>||</sup> Shuanghong Tian,<sup>\*,†,⊥</sup> and Ya Xiong<sup>\*,†,⊥</sup>

<sup>†</sup>School of Environmental Science and Engineering, Sun Yat-Sen University, Guangzhou 510275, People's Republic of China

<sup>‡</sup>Guangzhou Sewage Purification Co., Ltd., Guangzhou 510655, Guangdong, People's Republic of China

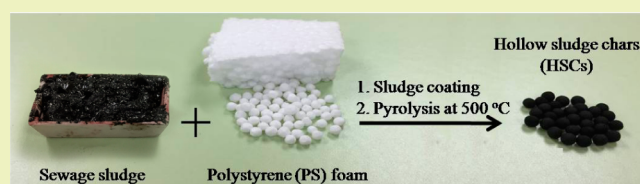
<sup>§</sup>School of Environmental Science and Engineering, Guangzhou University, Guangzhou 510275, People's Republic of China

<sup>||</sup>College of Science, South China Agriculture University, Guangzhou 510000, People's Republic of China

<sup>⊥</sup>Guangdong Provincial Key Laboratory of Environmental Pollution Control and Remediation Technology, Guangzhou 510275, People's Republic of China

**ABSTRACT:** Although sludge carbons have been widely studied, no attention has been paid to the preparation and application of hollow sludge carbon. In this study, innovative hollow spherical sludge carbons (HSCs) were prepared by pyrolyzing polystyrene foam sphere @sludge. The precursors, including sewage sludge and polystyrene foam, are solid wastes and produced in large volumes around the world. By this method, HSCs with a tunable shell thickness from 0.2 to 2.5 mm were obtained. The batch and column experiments show that the adsorption capacity and rate of HSCs for methylene blue increase with the decrease of the shell thickness, e.g., HSC with 0.2 mm thickness exhibits the highest adsorption capability of 149 mg g<sup>-1</sup> and intraparticle diffusion rate constant of 21.5 mg g<sup>-1</sup> h<sup>-0.5</sup>, 2.2 and 3.8 times larger than that of solid sludge carbon, respectively. In addition, two modification methods were proposed to further enhance the adsorption performance of HSCs. Finally, HSCs can be easily recycled and efficiently regenerated by thermal treatment. These results demonstrate that HSCs with thin shell thickness is a promising adsorbent for wastewater treatment and the production of HSCs is a sustainable strategy for beneficial use of sewage sludge and PS foam wastes.

**KEYWORDS:** Hollow sludge carbon, polystyrene foam waste, adsorption, methylene blue



## INTRODUCTION

Sewage sludge is an inevitable byproduct during wastewater treatment, which is produced in large volumes around the world. These huge amounts of waste materials, consequently, cause major handling and disposal problems.<sup>1</sup> The conventional disposal methods such as landfilling, agricultural use, and incineration have severe limitations with increasing environmental and legislative constraints.<sup>2</sup> In view of the high content of organic components in sewage sludge, carbonization of sludge to produce low-cost sludge carbon has emerged as a sustainable strategy for beneficial use of sewage sludge. This strategy can not only reduce sewage sludge but also turn solid waste into useful material for environment remediation.<sup>3</sup>

In recent years, sludge carbons with large specific surface areas and well-developed porosity have been widely reported to be used as adsorbents for the removal of organic and inorganic pollutants, and proven to be promising for environmental remediation.<sup>4–8</sup> However, these sludge carbons are employed in the form of powders. It is quite difficult to remove these powders from large volumes of water, which limits their practical application. Alternatively, the granular sludge carbons are easily separated from aqueous solution, but the interior carbons of these granularities act less due to the mass transfer limitation.<sup>9</sup> Therefore, it is very intriguing to develop an

innovative sludge carbon that presents easy separation and large adsorption capacity.

Hollow-structured porous spheres, featured with hollow cores and porous shells, have drawn increasing attention for their merits of low density, large void space, high surface area, and good permeability. These features make the hollow materials good candidates for drug delivery, photonics, gas sensor, catalysis, and adsorption to tackle environmental problems.<sup>10,11</sup> The literature has reported that hollow adsorbents presented higher adsorption capacity and rate in aqueous solution than solid counterparts.<sup>11–14</sup> These facts show that hollow adsorbents with thin porous shells are highly favorable to the adsorption process due to the shorter pathway for the mass diffusion to the inner surface. The shortened pore channels result in less diffusion blockage, which can enhance the utilization of the inner surface of the pores in the shell structure.<sup>10</sup> Hence, it is an interesting issue to fabricate a hollow spherical sludge carbon with a thin porous shell. To the best of our knowledge, there is no literature that reported the preparation and application of hollow sludge carbon.

**Received:** December 25, 2014

**Revised:** January 29, 2015

**Published:** February 4, 2015

Up to now, the most common and efficient method to fabricate a hollow architecture with a desired size has mainly involved the use of removable templates, referred to as hard templates, such as polymer latex,<sup>16</sup> silica,<sup>17</sup> and carbon spheres.<sup>18</sup> Among them, polystyrene (PS) latex sphere has been widely used as a hard template due to the well-defined and tunable particle size, and readily availability. With this approach, the hollow-core diameter can be easily adjusted by selecting different sized latexes, while the shell thickness can be tuned by varying the ratio of shell precursor-to-latex.<sup>19</sup> In the present study, we report the preparation of hollow spherical sludge carbon (HSC) via simply pyrolyzing PS@sewage sludge by using different sized polystyrene (PS) foam wastes as the sacrificial hard templates. As is well-known, the PS foam is widely used in packaging and is a major source of “white pollution”.<sup>20</sup> Production of HSCs by this method is also a sustainable strategy for beneficial use of PS foam wastes.

Herein, we report a fabrication strategy of hollow spherical sludge carbon (HSC) and the performance of HSCs as the adsorbent of organic pollutants in aqueous solution. These performances include adsorption capacity, adsorption kinetics, breakthrough kinetics, adsorption mechanism, thermal regeneration, etc. by batch and flow experiments. Special attention will be paid to investigate the dependence of these performances on the shell thickness of HSCs. The aim of these approaches is to develop a new product of sludge carbon with favorable features.

## EXPERIMENTAL SECTION

**Materials.** Dewater sewage sludge (SS) was obtained from the Datansha sewage treatment plant (Guangdong, China), and the chemical analysis of SS is shown in Table 1. The practical wastewater

**Table 1. Chemical Analysis of Sewage Sludge (SC) and the Hollow Sludge Carbon (HSC)**

sample	proximate analysis			elemental analysis		
	moisture (wt %)	ash (wt %)	volatiles (wt %)	C (%)	H (%)	N (%)
SS	78–80	44.6	56.2	22.9	4.0	4.4
HSC	0	27.9	72.1	18.7	1.7	1.5
hazardous elements (mg/kg dry SS or SC)						
As	Cd	Cr	Pb	Cu	Ni	
47.8	10.1	313.8	130.0	331.1	140.0	
10.1	1.1	93.0	27.2	140.2	49.8	

was collected from the influent and effluent sewage of the Datansha sewage treatment plant. Their COD concentrations were 265.8 and 48.8 mg L<sup>-1</sup>, respectively. Polystyrene spherical foams with diameters of 2.0, 3.5, and 4.8 mm were obtained from the commercially bought polystyrene foam package. Zinc chloride (ZnCl<sub>2</sub>, AR, Shanghai Chemical Co.), methylene blue (MB), and other reagents were all analytical grade and used as received without any further purification. Deionized water was used in all the experiments.

**Preparation of Hollow Spherical Sludge Carbons.** The hollow spherical sludge carbons were prepared according to the process shown in Figure 1. In an attempt to tune the shell thickness, polystyrene spherical foams with diameters of 2.0, 3.5, and 4.8 mm were used as the hard templates, which were then coated with the sludge pastes impregnated with ZnCl<sub>2</sub> in a ratio of 1:1, respectively. These spherical precursors with a controlling diameter of about 5 mm were dried at 105 °C to form a kind of PS@sludge sphere. The pyrolysis behavior of polystyrene foam from 200 to 600 °C was determined by a PerkinElmer 6300 thermogravimetric analyzer under a protective nitrogen atmosphere (200 mL min<sup>-1</sup>) at the heating rate

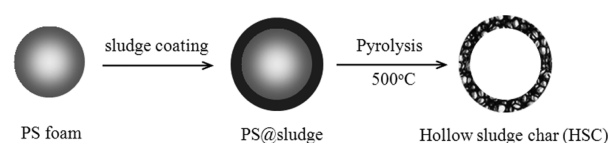


**Figure 1.** Schematic diagram of the preparation process of hollow spherical sludge chars (HSCs).

of 20 °C min<sup>-1</sup>. It was found that the polystyrene foam began to decompose at 350 °C and decomposed completely before 475 °C. Therefore, the obtained spheres were pyrolyzed at a rate of 20 °C min<sup>-1</sup> to 500 °C in the presence of N<sub>2</sub> holding for 2 h according to the reported preparation method for sludge char.<sup>21</sup> After cooling to room temperature, the products were washed with hydrochloric acid solution to remove inorganic compounds and then rinsed with deionized water until the pH reached 7.0. The obtained products were named as HSC2.0, HSC3.5, and HSC4.8, corresponding to the hard template with a diameter of 2.0, 3.5, and 4.8 mm. By using the same preparation method, solid spherical sludge carbon without using a template was also prepared and named as HSC0. For comparisons, the chemical analysis of HSC is shown in Table 1.

**Regeneration Experiments of the Adsorbent.** In an attempt to test the regeneration ability of the adsorbent, exhausted hollow spheres were regenerated by thermal treatment at 500 °C for 30 min under the protective N<sub>2</sub> atmosphere. Then the regenerated adsorbents were reused for further adsorption experiments.

**Characterization and Analytical Methods.** Element analysis of the obtained HSCs was conducted by an elemental analyzer (Vario EL, Elementar Co. Germany). Nitrogen adsorption isotherms were measured with an Autosorb-iQ-MP gas sorption analyzer (Quantachrome Instruments, USA) at 77 K. The Brunauer–Emmett–Teller (BET) method was utilized to calculate the specific surface areas ( $S_{\text{BET}}$ ) of the samples. The surface physical morphology of the sample was observed by the scanning electron microscopy (Hitachi S-2150, Japan). The X-ray diffraction (XRD) pattern of the prepared HSC was obtained by using D/max 2200 vpc diffractometer (Rigaku Corporation, Japan) with the Cu K $\alpha$  radiation at 40 kV and 30 mA. The mechanical properties of HSCs, including the impact resistance index (IRI) and abrasive resistance (AR), were also measured. The impact resistance was tested according to the ASTM method D440-86 of drop shatter for coal.<sup>22</sup> The BPs was dropped twice from 1.83 m onto a concrete floor. An impact resistance index (IRI) introduced by Richards was used to evaluate the impact resistance of the HSCs.<sup>23</sup> The IRI is calculated by  $\text{IRI} = (100N)/n$ , where  $N$  is the numbers of drops, and  $n$  is the total numbers of pieces after  $N$  drops. The abrasive resistance (AR) was tested according to the ASTM standard method D441-86 of tumbler test for coal.<sup>24</sup> In this test, three HSCs were placed in a porcelain jar. The jar was rotated at a speed of 200 rpm for 40 min. The weights of the HSCs before and after tumbling were measured and the weight loss was calculated as an indicator of the AR. The apparent density, also known as the bulk density, is an important characteristic of spherical activated carbon, being used for the determination of void fraction in packed column. The apparent density is measured according to the Chinese standard of GB/T 7702.4 27, where the specified samples filled into a column of a known volume are weighed and the apparent density of the sample can be given as the ratio of weighted mass to known volume.

**Adsorption Experiments.** The batch sorption experiment was performed in a glass Erlenmeyer flask with a stopper. In a typical run, the reaction suspension was prepared by adding a given amount of HSCs into MB solution with a pH value of 6.7. The flask containing the suspension was sonicated for 5 min and shaken in a reciprocating water-bath oscillator with a light shelter working at 25 °C and 200 rpm. Three mL of sample was taken at a given time interval from the flask to quantify adsorption.

The continuous adsorption was conducted in a fixed-bed column. It was made of a glass tube with an inner diameter of 1.1 cm and a height of 28.5 cm. The adsorbent (8.752 g) was packed in the column with the same bulk volume. MB solution with an initial concentration of

150 mg L<sup>-1</sup> and a pH value of 6.7 was pumped upward through the column at a desired flow rate controlled by a peristaltic pump (BL100-YZ15, PreFluid). The effluent of the column was collected at a certain time interval and the concentrations ( $C_t$ , mg/L) were measured using a UV-visible spectrophotometer (Shimadzu U2010, Japan) at 665 nm. The total adsorption quantity can be calculated by integrating the adsorbed concentration ( $C_0 - C_t$ , mg/L) versus  $t$  (h) plot.

## RESULTS AND DISCUSSION

**Characterization of Hollow Sludge Carbons.** Figure 2a presents the digital images of hollow spherical sludge carbons

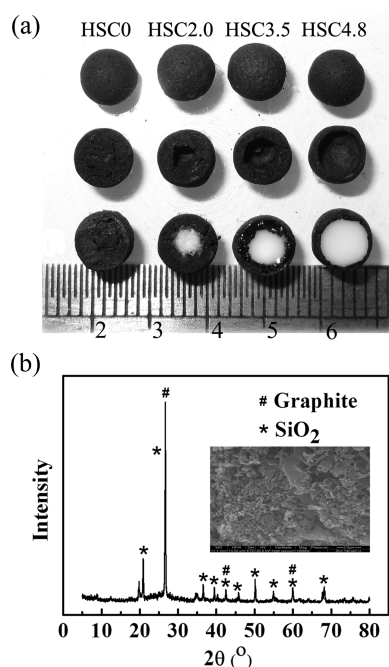


**Figure 2.** Characterization of HSCs. (a) Digital images of HSCs with different shell thickness; (b) XRD spectra of HSCs (inset is the SEM image of HSC shell).

produced from sewage sludge by using waste polystyrene foam as a sacrificial hard template. The outer diameter of all the precursors of HSCs, including PS@sludge spheres and the solid spheres without any template, is fixed at about 5 mm. After pyrolysis, the obtained HSCs maintain the spherical morphology with a similar average diameter as shown in the first row of Figure 2a. It is found that white PS foam disappeared completely and left a void or cavity in the sludge carbon, as shown in the second and third (the central white is the additional indicator) row of Figure 2a, which were artificially broken in order to conveniently observe the inner of these HSCs. The diameter of the inner void for HSC0, HSC2.0, HSC3.5, and HSC4.8 is about 0.0, 1.8, 3.2, and 4.5 mm, respectively, close to the diameter of the used hard templates (0.0, 2.0, 3.5, 4.8 mm). The shell thicknesses were measured to be about 2.5, 1.6, 0.9, and 0.2 mm, correspondingly. This indicates that both the size of inner void and the shell thickness can be easily tuned by employing variously sized hard template and controlling the outer diameter of PS@sludge spheres.

Moreover, the thinner shell wall is preferred if the spherical adsorbents are strong enough during the storage, transportation and application. Hence, the mechanical properties of HSCs, in terms of impact resistance index (IRI) and abrasive resistance (AR), were measured and displayed in Table 2. The low IRI

**Table 2.** Specific Area ( $S_{\text{BET}}$ ), Apparent Density and Mechanical Properties (IRI and AR) of HSCs

samples	$S_{\text{BET}}$ (m <sup>2</sup> /g)	apparent density (g/cm <sup>3</sup> )	IRI (%)	AR (%)
HSC0	344.4	0.3349	0.006	0
HSC2.0	342.7	0.3044	0.005	0
HSC3.5	352.7	0.2233	0.011	0
HSC4.8	370.0	0.0905	0.012	0
SC powder	376.2	0.3944		

values below 0.012% for all the HSCs indicate that HSCs are durable during storage and transportation. All the AR values are zero. It means no abrasion was detected and HSCs are very durable in the application of adsorption. These results show that even HSC4.8, with the largest size cavity and the thinnest shell wall, has enough mechanical strength to be used as adsorbents.

These HSCs with various shell thicknesses are all mainly composed of graphite carbon and SiO<sub>2</sub> (Figure 2b), and possess rich porous surface (inset of Figure 2b), slightly various surface areas (Table 2), but considerably different apparent densities. As shown in Table 2, the apparent densities decrease with the decrease of their shell thicknesses. For example, the apparent density of HSC4.8 with a shell thickness of 0.2 mm is 0.0905 g/cm<sup>3</sup>, only 27.0% that of the solid HSC0. The low apparent density will result in a less resistant loss in the filling adsorbent column and a large external surface. This is the advantage of the hollow spherical sludge carbon.

**Adsorption Performance of HSCs for MB.** The adsorption performance of HSC0, HSC2.0, HSC3.5, and HSC4.8 for MB was investigated by batch experiment, respectively. The adsorption capacity ( $q_t$ ) versus time was plotted in Figure 3. The adsorption capacity of all HSCs for

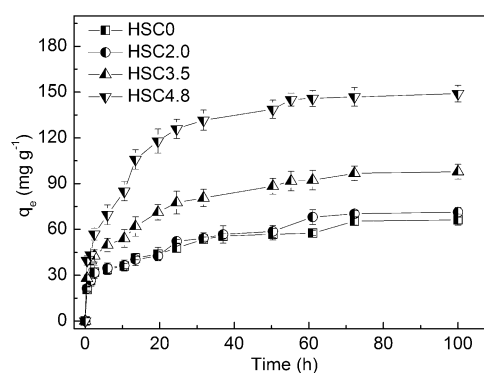


**Figure 3.** Adsorption kinetics of MB onto HSCs under the conditions of 172.5 mg L<sup>-1</sup> MB and 1.0 g L<sup>-1</sup> HSC.

MB shows a similar change tendency, that is, rapidly increases with the time and then slowly close to equilibrium. However, their quasi-equilibrium adsorption capacities depend on the shell thickness significantly. The quasi-equilibrium adsorption capacity of HSC4.8 with the thinnest shell (or the largest cavity) reaches 149.0 mg g<sup>-1</sup>, being 1.5, 2.1, and 2.2 times larger than that of HSC3.5, HSC3.0, and HSC0, respectively. It also outperforms many other carbon adsorbents derived from biomass solid waste.<sup>25</sup> Moreover, the adsorption capacities of HSCs per unite surface area showed the similar discrepancy. For example, the equilibrium adsorption capacity of HSC4.8 reached 0.40 mg m<sup>-2</sup>, being 1.4, 1.9, 2.1 times as much as that of HSC3.5, HSC3.0, and HSC0, respectively. Clearly, the data

further indicated that the difference of their adsorption capacity was mainly contributed to the difference of their shell thickness. It is noticed that the  $S_{\text{BET}}$  of HSCs are all close to that of SC powder and slightly affected by the shell thickness (Table 2), indicating that those HSCs have similar adsorption capacity to  $\text{N}_2$ . Herein adsorption capacities of HSCs to MB decreased significantly with the increase of the shell thickness, obviously different from the  $\text{N}_2$  adsorption. That is ascribed to the different molecular size of  $\text{N}_2$  and MB. The smaller  $\text{N}_2$  can penetrate into the sphere center independent of the shell thickness while MB encountered larger diffusion impedance during the transportation in the porous shell. The result shows that hierarchical pores containing micro-, meso-, and large levels in HSCs may be beneficial for the adsorption of MB since the low level pores can afford more surface for adsorption and the high level pores can help to mass transfer. Hence, simultaneously fabrication of micro-, meso-, and large pores could be one direction to further modify HSCs in the future work.

Adsorption is a multistep process and, due to the porosity of the particles, intraparticle diffusion is expected.<sup>26</sup> Thus, the intraparticle diffusion kinetic model based on the Weber–Morris equation (eq 1) is used to fit adsorption data in an attempt to describe the adsorption rate specifically and simultaneously demonstrate the adsorption mechanism.<sup>27</sup>

$$q_t = k_p t^{0.5} + c \quad (1)$$

where  $k_p$  ( $\text{mg g}^{-1} \text{h}^{-0.5}$ ) is the intraparticle diffusion rate constant, and  $c$  ( $\text{mg g}^{-1}$ ) is the constant proportional to the thickness of boundary layer, i.e., the larger the value of  $c$ , the greater the boundary layer thickness.

Figure 4a shows  $q_t$  versus  $t^{0.5}$  plot for the adsorption of MB on HSCs. If the intraparticle diffusion is the sole controlling process in adsorption, then the intraparticle diffusion plot should be linear and pass through the origin. But in the present case, the plots exhibit three-linearity in the time ranges of 0–0.5 h (not shown), 0.5–25 h, and 25–72 h for all HSCs, especially obviously for HSC4.8, indicating that the adsorption process is controlled by more than one process.<sup>26</sup> The first stage in 0–0.5 h indicates the instantaneous adsorption that mainly occurred on the external surface of adsorbents.<sup>15</sup> This stage is mainly due to the diffusion of the MB dye molecules through the film to the external surface of the adsorbent, so this process is very fast compared to those of the other two stages. The second stage is attributed to the slow intraparticle diffusion. The kinetic parameters of MB adsorbed onto HSCs in this stage are listed in Table 3. The relatively high values of  $R^2$  ( $>0.92$ ) suggests that the intraparticle diffusion played an important role in the adsorption process of MB adsorbed on HSCs. The larger value of  $k_p$  indicates the faster intraparticle adsorption. Herein the  $k_p$  follows the order of  $\text{HSC0} < \text{HSC2.0} < \text{HSC3.5} < \text{HSC4.8}$ , demonstrating that the thinner shell favors to the faster intraparticle adsorption. Moreover, HSC4.8 presented the highest reaction rate constant  $k_p$  of  $21.5 \text{ mg g}^{-1} \text{h}^{-1}$ , being 2.0, 3.6, and 3.8 times as much as that of HSC3.5, HSC3.0, and HSC0, respectively. There are two reasons to explain this result. On one hand, the hollow structures with thinner shell (or large size cavity) possess higher superficial surface per unit mass compared to their counterparts with thicker shell, which allow faster adsorption.<sup>28</sup> On the other hand, the thinner shell has shorter pathway for the MB diffusion and transport to the inner surface. As a result, the diffusion blockage in thinner shells

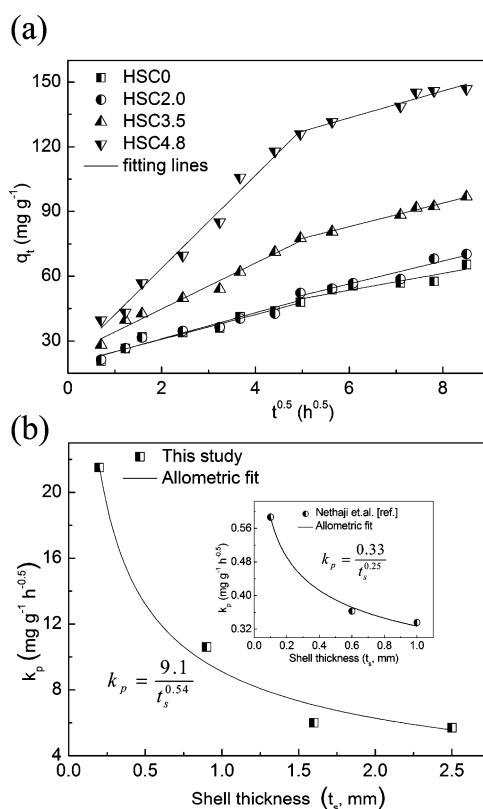


**Figure 4.** (a) Intraparticle diffusion kinetics plots for adsorption of MB onto HSCs. (b) Relationship of the intraparticle diffusion constant ( $k_p$ ) and the shell thickness ( $t_s$ ).

**Table 3. Comparison of Kinetic Parameters of MB Adsorbed onto HSCs**

adsorbent	intraparticle diffusion model		
	$k_p$ ( $\text{g mg}^{-1} \text{min}^{-0.5}$ )	$c$ ( $\text{mg g}^{-1}$ )	$R^2$
HSC0	5.7	20.9	0.982
HSC2.5	6.0	18.9	0.975
HSC3.5	10.6	26.8	0.929
HSC4.8	21.5	17.3	0.948

become less significant, MB can reach the inner surface of the pores relatively quickly and more inner surface area was utilized.<sup>10</sup> The third stage indicated that the intraparticle diffusion started to slow down due to the unavailability of active sites or the adsorbate molecules in the solution. In conclusion, the overall adsorption process of HSCs for MB was jointly controlled by external mass transfer and intraparticle diffusion.

To our best knowledge, adsorption research until now does not discuss the relationship of intraparticle diffusion constant ( $k_p$ ) and the thickness of the adsorbents ( $t_s$ ). Herein  $k_p$  versus  $t_s$  for HSCs is plotted in Figure 4b. To enrich the sampling data,  $k_p$  versus shell thickness  $t_s$  (i.e., radius) for the other solid spherical adsorbent reported in the literature was also plotted.<sup>29</sup> By nonlinear curve fitting, a similar trend that  $k_p$  has an allometric relationship with the shell thickness  $t_s$  was obtained. At the beginning,  $k_p$  decreased rapidly with the increase of shell thickness and then slowly. Even to some degree, further increasing the shell thickness would no longer affect the  $k_p$  value. That is probably due to that more channels are dead end in the very thick shell and thus the most inner surface can not be utilized. This kind of analysis reveals interesting relations

between intraparticle diffusion constant ( $k_p$ ) and shell thickness of the hollow spherical thickness. The present study highlights new possibilities for analyzing adsorption data. If similar analysis is routinely carried out by researchers, the results may possibly lead to better insight into the mechanism of adsorption.

The above experiments and analysis demonstrate that hollow adsorbents possess the advantages of high adsorption capacity and rate in the treatment of synthetic MB wastewater. Will these hollow adsorbents also show excellent performance in the actual wastewater treatment? To clarify this question, HSC4.8 with the thinnest shell and solid HSC0 were further used to treat the actual wastewater for comparisons. The influent and effluent sewage were collected from the Datansha sewage treatment plant and their COD concentrations were 265.8 and 48.8 mg L<sup>-1</sup>, respectively. Results show that 1.0 g/L HSC4.8 removed 82.6% COD from the influent sewage and 83.9% from the effluent sewage, about 2.2 and 1.7 times those of solid HSC0 with the same mass. In addition, the investigated effluent sewage met all indexes of landscape water except that the COD was beyond 30 mg L<sup>-1</sup> according to the national standard in China (Standard No.: GB/T 18921-2002). Because the remnant COD of the effluent sewage by HSC4.8 adsorption was as low as 7.9 mg L<sup>-1</sup>, it is obvious that the treated water can meet the COD requirement. Considering that the HSC derived from sewage sludge contains some hazardous elements as shown in Table 1, we sampled the treated water to analysis the leaching content of these hazardous elements by ICP. It was found that the concentrations of Cr, Pb, and Cd are too low to be detected due to the detection limit. It was noted that the leaching of Cu, Ni, and As, although it took place, remained below 0.01, 0.13, and 0.17 mg L<sup>-1</sup>, respectively, which is acceptable for scenic environment use according to the national standard in China (Standard No.: GB/T 18921-2002). (Cu < 1.0 mg L<sup>-1</sup>, Ni < 0.5 mg L<sup>-1</sup>, and As < 0.5 mg L<sup>-1</sup>). The results clarify that hollow spherical sludge carbon is also an efficient material for actual sewage treatment.

Column experiments were also conducted to determine the efficiency of HSCs with different shell thickness for removal of organic matter. HSC0, HSC2.0, HSC3.5, and HSC4.8 were used for the adsorption of MB in four fixed bed columns at the same adsorbent filling mass, respectively. Figure 5 shows their breakthrough curves using a plot of dimensionless concentration ( $C_t/C_0$ ) versus time ( $t$ ). With an increase in the shell thickness, the breakthrough curves shifts from left to right,

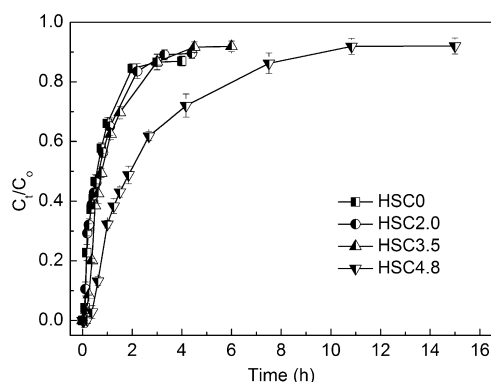


**Figure 5.** Adsorption breakthrough curves of HSCs to MB under the conditions of 172.5 mg L<sup>-1</sup> MB, flow rate of 303.72 mL h<sup>-1</sup>, and the adsorbent filling mass of about 8.8 g.

especially obviously for the most right curve of HSC4.8, which indicates that much more MB was removed by HSC4.8 because the integration area above the curve is the largest. It was also illustrated in Figure 5 that the half breakthrough time ( $t_{hb}$ ) at  $C_t/C_0$  of 0.5 was 33.8, 36.4, 42.9, and 60.7 min for HSC0, HSC2.0, HSC3.5, and HSC4.8, respectively. That can be explained by the fact that the bed height or effective adsorption zone presented the order HSC0 < HSC2.0 < HSC3.5 < HSC4.8 based on the same adsorbent filling mass due to the reverse order of their apparent densities shown in Table 2. At the larger bed height, breakthrough curve is dispersed and breakthrough occurs slower. In another word, the thinner shell of HSCs causes the less apparent density, and therefore the larger half breakthrough time. This can be contributed to the advantages of the hollow structure, i.e. the high utilization of surface and the efficient mass transfer.

The above results of both batch and column experiments show that the thinner shell of hollow adsorbents is helpful to enhance adsorption capacity and rate. However, the rate is still slow for MB molecules to diffuse into the most inner shell through micropores inside the particles. This makes us wonder if large channels in the shell can further promote the mass transfer and thereof enhance the adsorption performance. To demonstrate this case, the shell of HSC4.8 was modified by being punctured with a pin of 1 mm diameter. The adsorption performance of modified and unmodified HSC4.8 are compared in Figure 6. The adsorption curve of modified

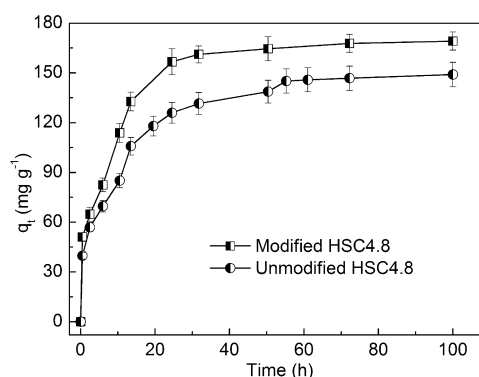


**Figure 6.** Adsorption performance of modified HSCs by fabricating a channel of 1 mm diameter in the shell under the conditions of 172.5 mg L<sup>-1</sup> MB and 1.0 g L<sup>-1</sup> adsorbent.

HSC4.8 obviously shifted to the positive direction of y-axis, implying that the adsorption capacity and the rate increased after this modification. That is because the solution can pass through the 1 mm large channels very quickly. In this way, MB molecules access the inner surface of shell more efficiently. It can be regarded that the MB molecules diffuse to the adsorption sites from both outer and inner shell simultaneously. This modification could of course further enhance the utilization of the inner surface and shorten the pathway of mass diffusion. Hence, fabrication of large channels in the shell proposes another direction to further modify HSCs.

**Thermal Regeneration of HSC4.8.** To be a promising adsorbent, HSCs should be readily recycled and regenerated. The millimeter HSCs can be easily recycled from the suspension by a conventional separation method, e.g., filtration. Herein the exhausted HSC4.8 adsorbents were regenerated by thermal treatment at 500 °C for 30 min. Considering that the adsorbed MB can be carbonized during the thermal

regeneration,  $\text{ZnCl}_2$  as a widely used pore-forming agent, was added in an attempt to fabricate new pores. The adsorption–regeneration cycle was repeated four times using the same experimental studies. The results of adsorption of MB onto virgin and regenerated HSC4.8 with or without  $\text{ZnCl}_2$  are shown in Figure 7. It can be seen that the adsorption amounts

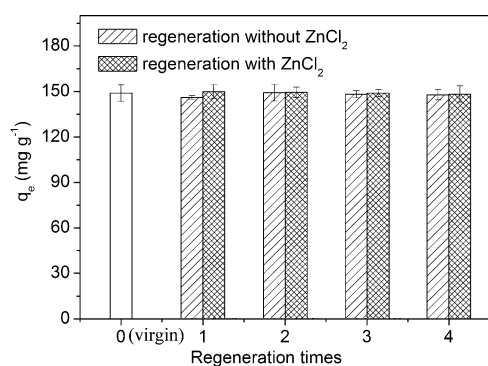


**Figure 7.** Adsorption capacity of HSC4.8 for MB at initial concentration of  $172.5 \text{ mg L}^{-1}$  after thermal regeneration.

at equilibrium are in the range of  $141\text{--}157 \text{ mg g}^{-1}$  for all the cycles. Obviously, the regeneration efficiency was close to 100% even after regeneration four times. This demonstrates that HSCs can be recycled at least four times without loss of adsorption capability and the thermal regeneration at  $500 \text{ }^\circ\text{C}$  for 30 min is quite effective. Furthermore, it seems like that the addition of  $\text{ZnCl}_2$  did not further enhance the adsorption capacity. That is because the quantity of adsorbed MB is too small to cause the observable change. Herein we presents a possibility to enhance the regeneration efficiency when much organic pollutants are adsorbed.

## CONCLUSIONS

Although sludge carbons have been widely studied, no attention has been paid on the preparation and application of hollow sludge carbon. In this work, innovative hollow spherical sludge carbons with tunable shell thickness from 0.2 to 2.5 mm have been successfully prepared by a sacrificial template method. The batch and column experiments show that the adsorption capacity and rate of HSCs for MB increased with the decrease of the shell thickness, and HSC with 0.2 mm thickness exhibited much higher adsorption capability and rate than the solid counterpart. Moreover, an interesting allometric relationship between intraparticle diffusion constant and shell thickness of HSCs has been revealed, which offers new possibilities for analyzing adsorption data. The strategy of fabricating hierarchical pores containing micro-, meso-, and large levels and even large channels in the shell was proposed to further modify HSCs. Finally, the millimeter HSCs can be easily recycled and efficiently regenerated by thermal treatment. These results demonstrate that hollow spherical sludge carbon is a promising adsorbent for practical wastewater treatment.

## AUTHOR INFORMATION

### Corresponding Authors

\*Tel.: +86-20-39332690. E-mail: t-sh-h@163.com or tshuangh@mail.sysu.edu.cn (Shuanghong Tian).

\*E-mail: cesxya@mail.sysu.edu.cn (Ya Xiong).

### Notes

The authors declare no competing financial interest.

## ACKNOWLEDGMENTS

This research was supported by Nature Science Foundations of China (21107146), Nature Foundations of Guangdong Province (92510027501000005), Science and Technology Research Programs of Guangzhou City (2012J4300118) and Project of Education Bureau of Guangdong Province (cgzhzd1001), and the Fundamental Research Funds for the Central Universities (121pgy20).

## REFERENCES

- (1) Chen, X. G.; Jeyaseelan, S.; Graham, N. Physical and chemical properties study of the activated carbon made from sewage sludge. *Waste Manage.* **2002**, *22*, 755–760.
- (2) Wang, F.; Shih, K.; Lu, X. W.; Liu, C. S. Mineralization behavior of fluorine in per-fluorooctanesulfonate (PFOS) during thermal treatment of lime-conditioned sludge. *Environ. Sci. Technol.* **2013**, *47*, 2621–2627.
- (3) Qian, T. T.; Jiang, H. Migration of phosphorus in sewage sludge during different thermal treatment processes. *ACS Sustainable Chem. Eng.* **2014**, *2*, 1411–1419.
- (4) Ros, A.; Montes-Moran, M. A.; Fuente, E.; Nevskaja, D. M.; Martin, M. J. Dried sludges and sludge-based chars for  $\text{H}_2\text{S}$  removal at low temperature: Influence of sewage sludge characteristics. *Environ. Sci. Technol.* **2006**, *40*, 302–309.
- (5) Wang, X. J.; Xu, X. M.; Liang, X.; Wang, Y.; Liu, M.; Wang, X.; Xia, S. Q.; Zhao, J. F.; Yin, D. Q.; Zhang, Y. L. Adsorption of copper(II) onto sewage sludge-derived materials via microwave irradiation. *J. Hazard. Mater.* **2011**, *192*, 1226–1233.
- (6) Athalathil, S.; Stueber, F.; Bengoa, C.; Font, J.; Fortuny, A.; Fabregat, A. Characterization and performance of carbonaceous materials obtained from exhausted sludges for the anaerobic biodecolorization of the azo dye Acid Orange II. *J. Hazard. Mater.* **2014**, *267*, 21–30.
- (7) Calisto, V.; Ferreira, C. I. A.; Santos, S. M.; Gil, M. V.; Otero, M.; Esteves, V. I. Production of adsorbents by pyrolysis of paper mill sludge and application on the removal of citalopram from water. *Bioresour. Technol.* **2014**, *166*, 335–344.
- (8) Kong, L. J.; Xiong, Y.; Sun, L. P.; Tian, S. H.; Xu, X. Y.; Zhao, C. Y.; Luo, R. S.; Yang, X.; Shi, K. M.; Liu, H. Y. Sorption performance and mechanism of a sludge-derived char as porous carbon-based hybrid adsorbent for benzene derivatives in aqueous solution. *J. Hazard. Mater.* **2014**, *274*, 205–211.
- (9) Liu, L. H.; Lin, Y.; Liu, Y. Y.; Zhu, H.; He, Q. Removal of methylene blue from aqueous solutions by sewage sludge based granular activated carbon: Adsorption equilibrium, kinetics, and thermodynamics. *J. Chem. Eng. Data* **2013**, *58*, 2248–2253.
- (10) Li, Y. S.; Shi, J. L. Hollow-structured mesoporous materials: Chemical synthesis, functionalization and applications. *Adv. Mater.* **2014**, *26*, 3176–3205.
- (11) Zhang, L. Z.; Jing, D. W.; Guo, L. J.; Yao, X. D. In situ photochemical synthesis of Zn-doped  $\text{Cu}_2\text{O}$  hollow microcubes for high efficient photocatalytic  $\text{H}_2$  production. *ACS Sustainable Chem. Eng.* **2014**, *2*, 1446–1452.
- (12) Wang, C.; Le, Y.; Cheng, B. Fabrication of porous  $\text{ZrO}_2$  hollow sphere and its adsorption performance to Congo red in water. *Ceram. Int.* **2014**, *40*, 10847–10856.
- (13) Wang, X.; Cai, X.; Shen, F. L.  $\text{TiO}_2$  hollow microspheres with mesoporous surface: Superior adsorption performance for dye removal. *Appl. Surf. Sci.* **2014**, *305*, 352–358.
- (14) Zhang, L. H.; Sun, Q.; Liu, D. H.; Lu, A. H. Magnetic hollow carbon nanospheres for removal of chromium ions. *J. Mater. Chem. A* **2013**, *33*, 9477–9483.
- (15) Guo, L.; Zhang, L.; Zhang, J.; Zhou, J.; He, Q.; Zeng, S.; Cui, X.; Shi, J. Hollow mesoporous carbon spheres - An excellent bilirubin adsorbent. *Chem. Commun.* **2009**, *40*, 6071–6073.
- (16) Liu, F. Q.; Li, W. H.; Liu, B. C.; Li, R. X. Synthesis, characterization, and high temperature  $\text{CO}_2$  capture of new CaO based hollow sphere sorbents. *J. Mater. Chem. A* **2013**, *1*, 8037–8044.

- (17) Alonso-Morales, N.; Gilarranz, M. A.; Palomar, J.; Lemus, J.; Heras, F.; Rodriguez, J. J. Preparation of hollow submicrocapsules with a mesoporous carbon shell. *Carbon* **2013**, *59*, 430–438.
- (18) Sawant, S. Y.; Somani, R. S.; Panda, A. B.; Bajaj, H. C. Utilization of plastic wastes for synthesis of carbon microspheres and their use as a template for nanocrystalline copper(II) oxide hollow spheres. *ACS Sustainable Chem. Eng.* **2013**, *1*, 1390–1397.
- (19) Tan, B.; Rankin, S. E. Dual latex/surfactant templating of hollow spherical silica particles with ordered mesoporous shells. *Langmuir*. **2005**, *21*, 8180–8187.
- (20) You, C. H.; Liao, S. J.; Qiao, X. C.; Zeng, X. Y.; Liu, F. F.; Zheng, R. P.; Song, H. Y.; Zeng, J. H.; Li, Y. W. Conversion of polystyrene foam to a high-performance doped carbon catalyst with ultrahigh surface area and hierarchical porous structure for oxygen reduction. *J. Mater. Chem. A* **2014**, *31*, 12240–12246.
- (21) Rozada, F.; Otero, M.; Morán, A.; García, A.I. Adsorption of heavy metals onto sewage sludge-derived materials. *Bioresour. Technol.* **2008**, *99*, 6332–6338.
- (22) D440-D486: Standard test method of drop shatter test for coal. *Annual Book of ASTM Standards*; American Society for Testing and Materials: West Conshohochon PA, 1998; pp 188–191.
- (23) Richards, S. R. Physical testing of fuel briquettes. *Fuel Proc. Technol.* **1990**, *25*, 89–100.
- (24) D441-D486: Standard test method of tumbler test for coal. *Annual Book of ASTM Standards*; American Society for Testing and Materials: West Conshohochon, PA, 1998; pp 192–194.
- (25) Yagub, M. T.; Sen, T. K.; Afroze, S.; Ang, H. M. Dye and its removal from aqueous solution by adsorption: A review. *Adv. Colloid. Interface Sci.* **2014**, *209*, 172–184.
- (26) Cheknane, B.; Zermane, F.; Baudu, M.; Bouras, O.; Basly, J. P. Sorption of basic dyes onto granulated pillared clays: Thermodynamic and kinetic studies. *J. Colloid Interface Sci.* **2012**, *381*, 158–163.
- (27) Weber, W. J.; Morris, J. C. *Proceedings of the International Conference on Water Pollution Symposium*; Pergamon: Oxford, U. K., 1962; Vol. 2, pp 231–266.
- (28) Jayaprakash, N.; Shen, J.; Moganty, S. S.; Corona, A.; Archer, L. A. *Angew. Chem., Int. Ed.* **2011**, *50*, 5904–5908.
- (29) Nethaji, S.; Sivasamy, A. Adsorptive removal of an acid dye by lignocellulosic waste biomass activated carbon: Equilibrium and kinetic studies. *Chemosphere* **2011**, *82*, 1367–1372.